Eur. Phys. J. D **27**, 33–41 (2003)
DOI: 10.1140/epjd/e2003-00235-1

THE EUROPEAN PHYSICAL JOURNAL D

Radiative lifetime measurements and oscillator strength determination for transitions in singly ionized praseodymium (Pr II)

E. Biémont[1,2,a], P.-H. Lefèbvre[2,b], P. Quinet[1,2,c], S. Svanberg[3,d], and H.L. Xu[3,e]

[1] Astrophysique et Spectroscopie, Université de Mons-Hainaut, 7000 Mons, Belgium
[2] IPNAS, Université de Liège, Sart Tilman B15, 4000 Liège, Belgium
[3] Department of Physics, Lund Institute of Technology, PO Box 118, 221 00 Lund, Sweden

Received 26 March 2003 / Received in final form 16 May 2003
Published online 29 July 2003 –

Abstract. New radiative lifetimes for 20 levels of Pr II have been measured using the time-resolved laser-induced fluorescence (LIF) technique. The combination of these experimental values with theoretical branching fractions (BF) obtained with the pseudo-relativistic Hartree-Fock (HFR) approach has allowed us to determine oscillator strengths and transition probabilities for about 150 lines appearing in the spectral region between 369.9 and 741.2 nm. A detailed discussion of our new results and comparisons with previous data are also given in the present paper.

PACS. 32.70.Cs Oscillator strengths, lifetimes, transition moments – 42.62.Fi Laser spectroscopy

1 Introduction

Pr II accurate transition probabilities are needed in astrophysics for solving problems related to high overabundances of this element observed in many types of stars like, *e.g.*, the A and B stars (see *e.g.* [1]) or the ultra-metal-poor giant stars (see, *e.g.* [2]). A detailed investigation of diffusive processes active in stellar atmospheres requires a large number of precise atomic data concerning both the line positions and strengths. However, in this ion, accurate atomic data for line intensities are available only for a limited number of transitions while many lines are observed in astrophysical objects. Pr II is indeed well represented in the photospheric solar spectrum (see *e.g.* [3,4]) and shows also numerous absorption features in the spectrum of F-type supergiants and of Ap or Am stars (see, *e.g.* [1,5]).

A review on the present state of the art regarding the atomic data of lanthanides, and of Pr ions in particular, has been published very recently [6].

Pioneering work regarding radiative parameter determination in singly ionized praseodymium includes the arc measurements of Corliss and Bozman [7] and the lifetime determinations by beam-foil spectroscopy of Andersen and Sorensen [8] and of Andersen *et al.* [9]. These results, however, suffer from well-known limitations of these techniques like departures from thermodynamic equilibrium in the first case, or non-selective excitation and Doppler-limited spectral resolution in the second approach.

Later on, determinations of transition probabilities were published by Lage and Whaling [10] who adopted the lifetime values obtained by Andersen *et al.* [8,9] for four levels and measured branching fractions in order to deduce A-values for 40 lines. More recently, Goly *et al.* [11] considered Pr II lines emitted from a ferroelectric plasma source in the range 200.0 to 700.0 nm and were able to deduce transition probabilities for 62 Pr II-lines. Additional lifetime measurements (14 levels) in this ion were made by Gorshkov and Komarovskii [12] using a delayed-coincidence technique. A compilation of the measurements available up to 1994 has been prepared by Blagoev and Komarovskii [13].

Very recently, 33 levels of Pr II were measured by Scholl *et al.* [14] using the beam-laser method with an accuracy in the range 1–11% and lifetime values between 6 and 170 ns. Transition probabilities have been proposed by these authors for 82 transitions of Pr II in the wavelength domain 392–640 nm. Similarly, radiative lifetimes for 11 levels of Pr II have been obtained by laser-induced fluorescence spectroscopy by Dolk *et al.* [1] and, combined with new branching fraction measurements, they have allowed us to refine the chemical composition of some HgMn stars.

The ionization equilibrium of astrophysical plasmas suggests that both singly ionized and doubly ionized praseodymium are expected to be present in the outer layers of many stars. A combination of theoretical branching fractions (deduced from HFR calculations including

[a] e-mail: E.Biemont@ulg.ac.be
[b] e-mail: ph.lefebvre@ulg.ac.be
[c] e-mail: Pascal.Quinet@umh.ac.be
[d] e-mail: Sune.svanberg@fysik.lth.se
[e] e-mail: Huailiang.Xu@fysik.lth.se

core-polarization effects) and of radiative lifetime measurements (obtained using the time-resolved LIF method) has appeared very successful recently in the case of Pr III [15] for getting reliable transition probabilities.

The present work, concerning singly charged praseodymium, appears as the logical and natural extension of the previous measurements and calculations in Pr III [15,16].

2 The singly-ionized praseodymium spectrum

Praseodymium is an odd lanthanide ($Z = 59$) having only one stable isotope ^{141}Pr. The nuclear spin $I = 5/2$ and the nuclear magnetic moment ($\mu = 4.136$) are large and this ion exhibits hyperfine structure particularly for the $4f^3 6s$–$4f^3 6p$ transitions, these effects being smaller for the $4f^3 5d$–$4f^3 6p$ lines (see *e.g.* [17–20]).

Unexpectedly, the Pr II spectrum is still very poorly known. In fact, when looking at the NIST compilation [21], one can observe that, for this ion, only 59 even-parity levels up to 35 497 cm^{-1} and 149 odd-parity levels up to 30 018 cm^{-1} have been established experimentally while theoretical predictions give rise to 385 possible even levels and 469 possible odd levels in the same energy regions.

The experimentally determined energy levels belong to the configurations $4f^3(^4\mathrm{I^o})6s$, $4f^3(^4\mathrm{I^o})5d$, $4f^2(^3\mathrm{H})5d^2$, $4f^2(^3\mathrm{H})5d6s$, $4f^3(^4\mathrm{I^o})6p$ and $4f^2(^3\mathrm{H})5d6p$ but, for many levels, the assignments are uncertain since the calculated mixings appear to be very important even for these low-lying configurations.

The high density of levels in this ion requires that special care must be taken to avoid possible blends in the spectrum and it could make a reliable least-squares fitting procedure for adjusting the Slater parameters illusory (see Sect. 4).

3 Lifetime measurements

Traditionally, in atomic spectra, transition probabilities can be derived from a combination of lifetime measurements with BF determinations using either experimental or theoretical approaches.

Among the methods available for lifetime measurements, a very reliable one is the selective excitation of a level of interest followed by direct observation of the exponential decay of the fluorescence released from that level. In the present work, the measurements were undertaken by using the time-resolved LIF technique. The Pr^+ ions were generated in a praseodymium plasma by laser ablation. The laser-induced plasma has the advantage of high ionic populations in ground as well as in metastable states that can be used as a starting point for laser excitation to upper levels. The ablation laser pulses used in the measurements were emitted from a Nd:YAG laser (Continuum Surelite), characterized by a 532-nm wavelength, a 10-ns duration, and a variable energy normally in the range 2–10 mJ. The pulses were focused vertically onto the surface of a rotating praseodymium foil, which was put into a vacuum chamber with a background pressure of about 10^{-6}–10^{-5} mbar. After the laser pulse has impinged on the pure praseodymium foil, a small plasma containing electrons, atoms and ions of various ionization stages was produced and expanded.

The levels of interest in Pr II were populated with a tunable, linearly polarized, pulsed visible and UV laser radiation of about 1 ns duration. An injection seeded and Q-switched Nd:YAG laser (Continuum NY-82) emitted laser pulses of 8 ns duration with 532 nm wavelength at a repetition rate of 10 Hz. The technique of stimulated Brillouin scattering (SBS) in water was used in the experiment to compress the laser pulse to about 1 ns. These compressed pulses were then employed to pump a dye laser, in which a DCM dye was operated. The radiation from the dye laser could be frequency doubled in a KDP crystal. The second harmonic of the dye laser radiation was then focused into a hydrogen gas cell with a pressure at about 10 bars, in which different orders of stimulated Stokes Raman scattering (SSRS) were obtained. The desired spectral range from 367 to 452 nm could be covered by this technique. A CaF_2 Pellin-Broca prism was employed to isolate the different components of the laser beams from the SSRS cell for obtaining the required excitation. The appropriate excitation light was sent horizontally into the vacuum chamber and crossed an extended plasma zone located about 10 mm above the rotating target surface. Details about the experimental device can be found elsewhere (see *e.g.* [22]).

Twenty even-parity levels in the energy range from 22 571 to 30 019 cm^{-1} were excited, with a single-step process, from the ground state and appropriate metastable states belonging to the configuration $4f^3 6s$. The excitation schemes used in the present experiment are reported in Table 1.

Synchronization of ablation and excitation pulses was achieved by external triggering from a digital delay generator (Stanford Research Systems Model 535). The delay times between the ablation and the excitation pulses varied between 2 and 5 μs perpendicularly to the laser radiation, the fluorescence due to the decay of the excited levels was collected by a fused-silica lens and focused into the entrance slit of a 1/8 m monochromator. In order to avoid possible errors in the level selection by the exciting laser light, the different possible decay channels from the excited levels to lower states were carefully checked for consistency.

The time-resolved fluorescence signal from a fast photomultiplier was recorded with a digitizing oscilloscope (Tektronix Model DSA 602). In the measurements, different fitting processes were adopted for the evaluation of the lifetimes. For the lifetimes longer than 10 ns, a least-squares exponential fitting procedure was applied to the decay at delays sufficient for the excitation pulses to vanish. For the lifetimes shorter than 10 ns, the temporal shape of the exciting laser pulses and the response function of the LIF detection were taken into account. The experimental fluorescence decay curve was fitted to a convolution of a pure exponential function and the excitation

Table 1. Pr II levels considered in the present work and corresponding excitation schemes.

E (cm^{-1})[a]	Origin (cm^{-1})	Dye laser λ $(nm)_{air.}$	Laser Mode[b]	Excitation λ $(nm)_{vac}$	Observed λ $(nm)_{vac}$
22571.48	441.95	656.859	2ω + 2S	451.88	452
22675.44	0.0	645.286	2ω + 2S	441.01	450
23261.36	0.0	633.309	2ω + 2S	429.89	430
23660.20	441.95	634.176	2ω + 2S	430.69	423
24115.50	441.95	625.148	2ω + 2S	422.41	445
24754.95	1743.72	638.368	2ω + 2S	434.57	404
25569.19	2998.36	647.471	2ω + 2S	443.04	418
25610.20	1649.01	619.576	2ω + 2S	417.34	397
25814.44	0.0	667.162	2ω + S	387.38	394
25842.41	1743.72	616.947	2ω + 2S	414.96	394
26226.56	0.0	658.112	2ω + S	381.29	388
26524.02	441.95	661.256	2ω + S	383.41	404
26860.95	2998.36	621.475	2ω + 2S	419.06	397
26961.96	441.95	651.816	2ω + S	377.07	395
26973.49	441.95	651.571	2ω + S	376.91	395
27128.00	2998.36	616.358	2ω + 2S	414.42	441
27198.24	0.0	637.716	2ω + S	367.67	391
28508.79	1649.01	644.675	2ω + S	372.30	398
29723.97	2998.36	647.476	2ω + S	374.17	406
30018.10	2998.36	641.368	2ω + S	370.09	401

[a] The energy level values are taken from the NIST compilation [21], [b] 2ω means the second harmonic, S and 2S are written for the first and second Stokes components of the Raman scattering.

pulse, which was recorded by inserting a metal rod into the interaction zone of the excitation laser and the plasma when the ablation beam was blocked. For each level investigated, a series of measurements, under different conditions, were performed to eliminate systematic errors, such as saturation effects, flight-out-of-view contributions, radiation trapping and collisional effects. It was found that the detected fluorescence intensity could be varied by a factor of 10 without altering the lifetime values (within the statistical scattering).

The flight-out-of-view effects were specially considered for the longer lifetimes and minimized by adjusting the position and width of the entrance slit of the monochromator and the delay times between the ablation and the excitation pulses. Still, larger error bars have been given for the longer lifetimes because the speeds of Pr^+ ions are larger than those of Pr atoms.

In addition, a static magnetic field of about 100 Gauss, provided by a pair of Helmholtz coils, was added or removed over the interaction zone to check possible quantum beats due to the Zeeman effect for long-lived states. The 20 experimental lifetimes of Pr II measured in the present work are given in Table 2, where they are compared with the previously available results and with the theoretical HFR values obtained in the present work according to the procedure described in the following section.

4 Theoretical approach

The theoretical method considered in this paper is the well established HFR approach described by Cowan [23]. Configuration interaction was explicitly retained among the $4f^36s$, $4f^35d$, $4f^36d$, $4f^25d6p$, $4f^26s6p$, $4f5d^3$, $4f5d^26s$ and $4f5d6s^2$ odd-parity configurations and among the $4f^36p$, $4f^35f$, $4f^4$, $4f^25d^2$, $4f^26s^2$, $4f^26p^2$, $4f^25d6s$, $4f5d^26p$ and $4f5d6s6p$ even-parity configurations. These configuration lists are expected to include the most important effects due to intravalence and core-valence

Table 2. Experimental and theoretical radiative lifetimes in Pr II obtained in the present work and comparison with previous measurements.

E_{exp} [a] (cm^{-1})	τ_{exp} [b] (ns)	$\tau_{previous}$ (ns)	E_{HFR} [b] (cm^{-1})	τ_{HFR} [b] (ns)
22571.48	51(4)	51.8(6)[g]	22620	121
22675.44	13.5(6)	15(1.5)[e], 13.0(1.1)[f], 13.5(2)[g]	22770	6.2
23261.36	48.3(2.0)	48.8(1.6)[g]	23432	55.9
23660.20	7.3(0.4)	11(2)[e], 7.57(15)[g]	23545	12.1
			23694	11.4
24115.50	7.5(0.4)	12(2)[e], 7.92(15)[g]	24153	5.2
24754.95	37(3)		25192	34.7
25569.19	6.1(3)	7.8(1.0)[c], 8.4(1.0)[e], 6.0(3)[f], 6.32(39)[g]	25708	5.9
25610.20	21.5(1.5)	21.1(5)[g]	25037	26.7
25814.44	125(15)		25704	94.2
25842.41	45(3)		26197	51.5
26226.56	12.4(6)		26044	10.1
26524.02	77(7)		26995	78.6
26860.95	6.7(3)	15(1.5)[e], 7.0(4)[f], 6.69(52)[g]	27069	7.5
26961.96	11.8(0.6)	11.7(5)[g]	26549	13.2
			26702	14.3
26973.49	18.0(1.5)		26747	19.7
27128.00	5.6(3)	8.4(1.2)[c], 8.4(1.2)[d], 10(2)[e], 5.5(3)[f], 5.79(13)[g]	27248	4.6
27198.24	15.3(1.0)		27164	8.6
			27493	12.4
28508.79	5.6(4)		27941	9.1
			28615	9.0
			28807	8.4
29723.97	6.0(3)		29937	6.5
30018.10	5.3(3)		30351	4.7

[a] From NIST compilation [21], [b] this work, [c] [8] (beam-foil spectroscopy), [d] [9] (beam-foil spectroscopy), [e] [12] (delayed coincidence method), [f] [1] (laser induced fluorescence technique), [g] [14] (beam-laser method).

correlation. Consequently, no additional core-polarization pseudo-potential was introduced in the physical model.

In view of the scarcity of experimentally determined energy levels available in Pr II, no semi-empirical adjustment of the radial parameters could be seriously considered. Instead, in order to obtain a more realistic representation of the Pr II energy spectrum, all the Slater integrals were scaled down by a factor 0.75, a rather low factor as recommended by Cowan [23] and the average energies were adjusted to reproduce adequately the levels given in the NIST compilation [21] or predicted by Brewer [24] for the lowest level of each configuration, *i.e.* $4f^36s\ ^5I_4$ ($E = 0$ cm^{-1}), $4f^35d\ ^5L_6$ ($E = 3\,893$ cm^{-1}), $4f^25d6p\ ^5L_6$ ($E = 31\,000 \pm 2\,000$ cm^{-1}), $4f^26s6p\ ^5I_4$ ($E = 39\,500 \pm 2\,000$ cm^{-1}), $4f5d^3\ ^5I_4$ ($E = 57\,000 \pm 4\,000$ cm^{-1}), $4f5d^26s\ ^5H_3$ ($E = 55\,000 \pm 4\,000$ cm^{-1}), $4f5d6s^2\ ^3H_4$ ($E = 67\,000 \pm 3\,000$ cm^{-1}), $4f^36p\ ^5K_5$ ($E = 22\,675$ cm^{-1}), $4f^4\ ^5I_4$ ($E = 32\,000 \pm 2\,000$ cm^{-1}), $4f^25d^2\ ^5L_6$ ($E = 5\,855$ cm^{-1}), $4f^26s^2\ ^3H_4$ ($E = 16\,000 \pm 2\,000$ cm^{-1}), $4f^26p^2\ ^5I_4$ ($E = 68\,000 \pm 2\,000$ cm^{-1}), $4f^25d6s\ ^5K_5$ ($E = 7\,888$ cm^{-1}), $4f5d^26p\ ^5K_5$ ($E = 83\,000 \pm 6\,000$ cm^{-1}) and $4f5d6s6p\ ^5I_4$ ($E = 91\,000 \pm 4\,000$ cm^{-1}). For the configurations $4f^36d$ and $4f^35f$, for which no predictions were provided by Brewer [24], the average energies were increased by 22 000 cm^{-1} by analogy with similar configurations, *i.e.* $4f^36s$, $4f^35d$ and $4f^36p$.

5 Discussion of the results

HFR and experimental lifetimes obtained in the present work are compared with previous measurements in Table 2. These measurements were due to Andersen *et al.* [8,9], Gorshkov and Komarovskii [12], Dolk *et al.* [1] and Scholl *et al.* [14].

When looking at the table, one can observe that our new experimental values are 22 and 33% shorter than the beam-foil measurements of Andersen *et al.* [8,9] for the two levels situated at 25 569.19 cm^{-1} and 27 128.00 cm^{-1}, respectively. Larger disagreements, reaching even a factor of 2 for the levels at 26 860.95 cm^{-1} and 27 128.00 cm^{-1}, are observed when comparing the lifetimes obtained in the present work with the delayed-coincidence measurements of Gorshkov and Komarovskii [12]. However, an excellent agreement (within the errors) is found, for the same levels, between our measurements and the accurate laser measurements recently published by Dolk *et al.* [1] and Scholl *et al.* [14]. The same excellent agreement is observed for

Table 3. Even-parity energy in Pr II for which radiative lifetimes have been measured in the present work.

E_{exp}[a] (cm^{-1})	g_{exp}[a]	Config.[a]	Term[a]	J	E_{HFR}[b] (cm^{-1})	g_{HFR}[b]	Leading components[b,c]
22571.48	1.166	?	?	5	22620	1.145	20% $4f^2(^3F)5d6s\ ^3G$ + 10% $4f^2(^3F)5d6s\ ^3G$ + 6% $4f^2(^3F)5d6s\ ^5F$
22675.44	0.830	$4f^3(^4I)6p$	^5K	5	22770	0.731	72% $4f^3(^4I)6p\ ^5K$ + 5% $4f^3(^4I)6p\ ^3I$ + 3% $4f^2(^3F)5d^2\ ^3I$
23261.36	0.920	?	?	5	23432	0.981	15% $4f^2(^3F)5d^2\ ^3I$ + 11 % $4f^2(^3H)5d^2\ ^3G$ + 11 % $4f^2(^3F)5d^2\ ^3I$
23660.20	0.67	$4f^3(^4I)6p$	^5I	4	23545	0.853	32% $4f^3(^4I)6p\ ^5I$ + 7% $4f^2(^3H)5d^2\ ^3H$ + 3% $4f^2(^1G)5d^2\ ^1G$
					23694	0.824	37% $4f^3(^4I)6p\ ^5I$ + 11% $4f^2(^3F)5d^2\ ^1G$ + 9% $4f^2(^3H)5d^2\ ^3H$
24115.50	0.959	$4f^3(^4I)6p$	^5K	6	24153	0.918	88% $4f^3(^4I)6p\ ^5K$ + 2% $4f^3(^4I)6p\ ^3I$ + 1% $4f^3(^2H)6p\ ^3I$
24754.95	0.908	?	?	4	25192	0.922	16% $4f^2(^3F)5d6s\ ^3H$ + 8% $4f^2(^1G)5d^2\ ^3H$ + 6% $4f^3(^4I)6p\ ^3H$
25569.19	1.07	$4f^3(^4I)6p$	^5K	7	25708	1.052	78% $4f^3(^4I)6p\ ^5K$ + 11 % $4f^2(^1G)5d^2\ ^1K$ + 2% $4f^2(^3H)5d^2\ ^3I$
25610.20	1.118	?	?	6	25037	0.980	22% $4f^2(^3F)5d^2\ ^3I$ + 15 % $4f^3(^4I)6p\ ^3K$ + 12 % $4f^2(^3F)5d^2\ ^3K$
25814.44	0.95	?	?	4	25704	1.084	11% $4f^2(^3F)5d^2\ ^5D$ + 8% $4f^2(^1G)5d^2\ ^3H$ + 6% $4f^2(^3F)5d^2\ ^3G$
25842.41	1.000	?	?	5	26197	1.041	17% $4f^2(^1G)5d^2\ ^3H$ + 14 % $4f^2(^3F)5d6s\ ^3H$ + 5% $4f^2(^3H)5d^2\ ^3H$
26226.56	0.91	$4f^3(^4I)6p$?	?	4	26044	0.909	26% $4f^3(^4I)6p\ ^5H$ + 14% $4f^2(^3F)5d^2\ ^3H$ + 8% $4f^2(^1D)5d^2\ ^3H$
26524.02	1.02	?	?	6	26995	1.123	30% $4f^2(^3H)5d^2\ ^3H$ + 12% $4f^2(^1G)5d^2\ ^3H$ + 9% $4f^2(^3F)5d^2\ ^3I$
26860.95	1.119	$4f^3$(4I)6p	^5I	7	27069	1.124	48% $4f^3(^4I)6p\ ^5I$ + 12% $4f^2(^3F)5d^2\ ^3K$ + 7% $4f^2(^3F)5d^2\ ^3I$
26961.96	1.076	?	?	6	26549	1.001	22% $4f^3(^4I)6p\ ^3K$ + 14 % $4f^2(^1G)5d^2\ ^1I$ + 14% $4f^3(^4I)6p\ ^5I$
					26702	1.008	15% $4f^3(^4I)6p\ ^3K$ + 11 % $4f^3(^4I)6p\ ^5I$ + 7% $4f^2(^3F)5d^2\ ^3I$
26973.49	1.11	?	?	5	26747	1.075	11% $4f^3(^4I)6p\ ^3I$ + 10% $4f^2(^3F)5d^2\ ^3G$ + 4% $4f^2(^3F)5d^2\ ^3G$
27128.00	?	$4f^3(^4I)6p$	^5K	8	27248	1.152	97% $4f^3(^4I)6p\ ^5K$ + 1% $4f^3(^2K)6p\ ^3L$ + 1% $4f^3(^4I)6p\ ^5I$
27198.24	1.07	$4f^3(^4I)6p$?	?	5	27164	1.047	31% $4f^3(^4I)6p\ ^5H$ + 12% $4f^2(^3F)5d^2\ ^3H$ + 7% $4f^2(^1D)5d^2\ ^3H$
					27493	1.042	24% $4f^3(^4I)6p\ ^5H$ + 17% $4f^2(^3F)5d^2\ ^3H$ + 6% $4f^2(^3F)5d^2\ ^3I$
28508.79	1.11	$4f^3(^4I)6p$	^3I	6	27941	1.087	21% $4f^3(^4I)6p\ ^3I$ + 18% $4f^3(^4I)6p\ ^5H$ + 7% $4f^2(^3F)5d^2\ ^3I$
					28615	1.123	23% $4f^3(^4I)6p\ ^5H$ + 14% $4f^3(^4I)6p\ ^3I$ + 13% $4f^2(^3F)5d^2\ ^3H$
					28807	1.103	25% $4f^3(^4I)6p\ ^5H$ + 15% $4f^3(^4I)6p\ ^3I$ + 10% $4f^2(^3F)5d^2\ ^3H$
29723.97	1.15	$4f^3(^4I)6p$?	?	8	29937	1.149	51% $4f^3(^4I)6p\ ^3K$ + 21 % $4f^3(^4I)6p\ ^5I$ + 10% $4f^2(^1I)5d^2\ ^3K$
30018.10	1.215	$4f^3(^4I)6p$	^5H?	7	30351	1.193	41% $4f^3(^4I)6p\ ^3I$ + 34% $4f^3(^4I)6p\ ^5H$ + 4% $4f^2(^1I)5d^2\ ^3I$

[a] From NIST compilation [21], [b] present work, [c] only the three main components are given.

all the other levels considered within the last two sets of data.

Looking at the theoretical results, it is worth mentioning that most of the levels reported in Table 2 are characterized by very strong mixings as illustrated in Table 3. These strong mixings can lead to difficulties in establishing the correspondence between experimental and theoretical level values. This is the case for the levels situated at 23 660.20, 26 961.96, 27 198.24 and 28 508.79 cm^{-1}, for which it was impossible to find with certainty the corresponding HFR values. Even when comparing the available Landé factors, it was not possible to label unambiguously these levels (see Col. 7 of Tab. 3).

For the 16 remaining levels, a very good agreement has been found between the HFR lifetimes and the laser measurements obtained in the present work if we except the levels at 22 571.48 and 22 675.44 cm^{-1} for which discrepancies reaching a factor of 2 were found between theory and experiment. These disagreements are attributed to the strong mixing and to inaccurate eigenvalue compositions. More accurate results for these two levels would require larger expansion sets for the wavefunctions but further investigations in that direction were prevented basically by computer limitations.

When excluding these latter two levels, the mean ratio between calculated and experimental lifetimes τ_{HFR}/τ_{exp} was found to be 0.98 ± 0.16 where the uncertainty represents the standard deviation from the mean.

In Table 4, calculated oscillator strengths and transition probabilities are given for the strongest lines ($\log gf > -2.0$) depopulating some of the levels for which radiative lifetimes were measured in the present work.

Table 4. Calculated oscillator strengths ($\log gf$ and transition probabilities (gA in s^{-1}) for selected transitions in Pr II. Only transitions with $\log gf > -2.00$ are given in the table. $A(B)$ stands for $A \times 10^B$.

λ[a]	Lower level[b]		Upper level[b]		log gf	gA	log gf	gA
(nm)	cm^{-1}	J	cm^{-1}	J	HFR[c]	HFR[c]	NORM[d]	NORM[d]
369.9945	2998	7	30018	7	–1.64	1.12(7)	–1.69	9.93(6)
374.0666	2998	7	29724	8	–1.45	1.70(7)	–1.41	1.84(7)
381.1847	0	4	26227	4	–0.64	1.04(8)	–0.73	8.47(7)
386.8511	0	4	25842	5	–1.85	6.53(6)	–1.79	7.47(6)
387.2703	0	4	25814	4	–1.38	1.83(7)	–1.50	1.38(7)
387.7183	442	5	26227	4	0.16	6.34(8)	0.07	5.16(8)
390.8052	4437	8	30018	7	0.42	1.14(9)	0.37	1.01(9)
393.5822	442	5	25842	5	–0.95	4.97(7)	–0.89	5.69(7)
394.0161	442	5	25814	4	–0.86	5.91(7)	–0.98	4.45(7)
394.7631	1649	6	26973	5	–0.63	9.64(7)	–0.59	1.06(8)
395.3510	4437	8	29724	8	0.21	6.82(8)	0.25	7.39(8)
396.2450	1744	5	26973	5	–0.13	3.04(8)	–0.09	3.33(8)
396.5253	1649	6	26861	7	–0.19	2.74(8)	–0.14	3.07(8)
397.2136	442	5	25610	6	–1.31	1.97(7)	–1.22	2.45(7)
400.8691	5079	7	30018	7	0.57	1.50(9)	0.51	1.33(9)
401.8963	1649	6	26524	6	–1.04	3.83(7)	–1.03	3.91(7)
403.4324	1744	5	26524	6	–1.10	3.33(7)	–1.09	3.40(7)
403.8455	0	4	24755	4	–0.78	7.06(7)	–0.81	6.62(7)
405.6535	5079	7	29724	8	0.56	1.43(9)	0.59	1.55(9)
408.3341	1744	5	26227	4	–1.29	1.98(7)	–1.38	1.61(7)
411.1866	442	5	24755	4	–0.52	1.24(8)	–0.54	1.16(8)
413.2193	1649	6	25842	5	–0.65	8.96(7)	–0.59	1.03(8)
414.3112	2998	7	27128	8	0.79	2.33(9)	0.70	1.91(9)
414.8433	1744	5	25842	5	–1.15	2.81(7)	–1.09	3.22(7)
417.9393	1649	6	25569	7	0.53	1.28(9)	0.51	1.24(9)
418.8796	1744	5	25610	6	–0.10	2.82(8)	–0.01	3.50(8)
418.9479	2998	7	26861	7	0.53	1.26(9)	0.57	1.41(9)
422.2934	442	5	24116	6	0.45	1.06(9)	0.29	7.35(8)
424.1437	3403	6	26973	5	–0.81	5.49(7)	–0.77	6.01(7)
424.9481	2998	7	26524	6	–1.12	2.81(7)	–1.12	2.87(7)
429.7766	0	4	23261	5	–0.64	8.33(7)	–0.58	9.64(7)
432.3892	3403	6	26524	6	–1.17	2.43(7)	–1.16	2.48(7)
434.4483	1744	5	24755	4	–1.18	2.39(7)	–1.21	2.24(7)
438.1003	442	5	23261	5	–0.99	3.60(7)	–0.93	4.17(7)
440.5825	4437	8	27128	8	–0.35	1.51(8)	–0.43	1.24(8)
442.1220	2998	7	25610	6	–1.67	6.76(6)	–1.58	8.40(6)
442.9253	2998	7	25569	7	–0.30	1.67(8)	–0.32	1.62(8)
444.9824	1649	6	24116	6	–0.11	2.61(8)	–0.27	1.81(8)
445.8296	4437	8	26861	7	–1.02	3.12(7)	–0.97	3.49(7)
446.8663	1744	5	24116	6	0.12	4.31(8)	–0.04	2.99(8)
447.1349	7660	8	30018	7	–1.60	8.20(6)	–1.66	7.27(6)
450.1824	3403	6	25610	6	–0.50	9.45(7)	–0.41	1.17(8)
451.0153	3403	6	25569	7	–0.01	3.12(8)	–0.03	3.02(8)
453.4154	5079	7	27128	8	–0.39	1.26(8)	–0.48	1.03(8)
456.1107	7806	9	29724	8	–1.81	4.86(6)	–1.78	5.26(6)
459.7054	5227	6	26973	5	–1.61	7.46(6)	–1.57	8.16(6)
462.5688	1649	6	23261	5	–1.36	1.37(7)	–1.29	1.59(7)
464.6049	1744	5	23261	5	–1.37	1.31(7)	–1.31	1.52(7)
466.1858	5079	7	26524	6	–1.82	4.62(6)	–1.81	4.72(6)
473.0827	4437	8	25569	7	–1.99	2.95(6)	–2.01	2.85(6)
473.4165	2998	7	24116	6	–1.96	3.18(6)	–2.12	2.20(6)
481.4339	8958	9	29724	8	–0.74	5.13(7)	–0.70	5.56(7)
482.6288	6414	7	27128	8	–1.34	1.27(7)	–1.43	1.04(7)
482.7197	6418	8	27128	8	–1.09	2.28(7)	–1.18	1.87(7)
483.9540	4098	5	24755	4	–1.88	3.91(6)	–1.90	3.67(6)
487.6258	5108	7	25610	6	–1.15	1.86(7)	–1.06	2.31(7)
487.9105	5079	7	25569	7	–1.57	7.31(6)	–1.58	7.07(6)
488.6032	5108	7	25569	7	–1.17	1.89(7)	–1.18	1.83(7)
489.0255	6418	8	26861	7	–1.12	2.11(7)	–1.07	2.36(7)
490.4516	5227	6	25610	6	–1.80	4.03(6)	–1.71	5.00(6)
491.4403	5227	6	25569	7	–1.45	9.74(6)	–1.46	9.42(6)
494.3720	3893	6	24116	6	–1.20	1.73(7)	–1.36	1.20(7)

Table 4. *Continued.*

λ[a] (nm)	Lower level[b] cm^{-1}	J	Upper level[b] cm^{-1}	J	log gf HFR[c]	gA HFR[c]	log gf (nm)	gA cm^{-1}
499.4136	4098	5	24116	6	–1.49	8.50(6)	–1.65	5.89(6)
500.1659	10030	7	30018	7	–1.82	3.84(6)	–1.88	3.41(6)
503.4312	3403	6	23261	5	–1.62	6.24(6)	–1.55	7.22(6)
507.6361	10030	7	29724	8	–1.92	2.93(6)	–1.89	3.17(6)
511.7523	7438	5	26973	5	–1.62	5.60(6)	–1.58	6.13(6)
513.5140	7660	8	27128	8	0.03	2.60(8)	–0.06	2.14(8)
516.1744	3893	6	23261	5	–1.07	2.18(7)	–1.00	2.52(7)
517.3902	7806	9	27128	8	0.49	7.50(8)	0.41	6.16(8)
518.3033	10730	6	30018	7	–1.97	2.53(6)	–2.02	2.24(6)
520.6561	7660	8	26861	7	–0.07	2.03(8)	–0.02	2.27(8)
521.9045	6414	7	25569	7	–0.14	1.76(8)	–0.15	1.70(8)
522.0108	6418	8	25569	7	0.34	5.25(8)	0.32	5.08(8)
525.9728	5108	7	24116	6	0.34	5.26(8)	0.19	3.65(8)
529.2619	5227	6	24116	6	–0.12	1.76(8)	–0.28	1.22(8)
532.0972	7438	5	26227	4	–0.96	2.35(7)	–1.05	1.91(7)
537.4971	11419	7	30018	7	–1.89	2.94(6)	–1.94	2.61(6)
540.8692	8490	5	26973	5	–1.67	4.50(6)	–1.63	4.92(6)
540.9081	7744	3	26227	4	–1.49	6.76(6)	–1.58	5.51(6)
543.1191	11611	8	30018	7	–1.70	4.31(6)	–1.75	3.82(6)
543.2038	7438	5	25842	5	–1.43	8.14(6)	–1.37	9.32(6)
544.0306	7438	5	25814	4	–1.73	3.87(6)	–1.85	2.92(6)
547.2349	11749	6	30018	7	–1.30	1.09(7)	–1.35	9.67(6)
551.5149	8100	4	26227	4	–0.69	4.05(7)	–0.78	3.30(7)
551.9388	11611	8	29724	8	–1.17	1.40(7)	–1.13	1.52(7)
554.3284	5226	6	23261	5	–1.66	4.77(6)	–1.59	5.52(6)
562.4441	12243	7	30018	7	–0.04	1.80(8)	–0.09	1.60(8)
563.6466	8490	5	26227	4	–1.26	1.06(7)	–1.35	8.63(6)
564.3456	8100	4	25814	4	–1.71	3.74(6)	–1.83	2.82(6)
568.1901	9379	5	26973	5	–0.93	2.16(7)	–0.89	2.36(7)
571.9080	12243	7	29724	8	–0.65	4.22(7)	–0.61	4.57(7)
575.3015	8465	6	25842	5	–1.33	9.18(6)	–1.27	1.05(7)
576.1247	8490	5	25842	5	–1.81	3.03(6)	–1.75	3.47(6)
576.9799	9647	6	26973	5	–1.30	9.07(6)	–1.26	9.93(6)
577.3164	7438	5	24755	4	–1.41	7.57(6)	–1.44	7.10(6)
580.7520	9647	6	26861	7	–1.41	7.26(6)	–1.36	8.13(6)
581.5331	12827	6	30018	7	–1.45	7.34(6)	–1.50	6.51(6)
581.8580	9045	3	26227	4	–0.66	3.88(7)	–0.75	3.16(7)
584.4914	8465	6	25569	7	–1.57	4.97(6)	–1.58	4.81(6)
584.7122	10030	7	27128	8	–0.95	2.05(7)	–1.03	1.68(7)
588.4527	13029	8	30018	7	–0.80	3.01(7)	–0.85	2.67(7)
593.0660	10117	4	26973	5	–1.06	1.46(7)	–1.02	1.60(7)
593.3803	9379	5	26227	4	–1.82	2.56(6)	–1.91	2.09(6)
593.9899	10030	7	26861	7	–0.33	8.38(7)	–0.28	9.38(7)
594.7185	10163	6	26973	5	–0.94	1.97(7)	–0.90	2.16(7)
596.1577	9045	3	25814	4	–1.69	3.47(6)	–1.82	2.61(6)
598.1444	9129	4	25842	5	–1.44	6.46(6)	–1.38	7.39(6)
598.7269	10163	6	26861	7	–1.10	1.42(7)	–1.05	1.59(7)
598.8202	13029	8	29724	8	–1.08	1.49(7)	–1.05	1.61(7)
599.4525	7438	5	24116	6	–1.69	3.51(6)	–1.85	2.43(6)
600.2457	8100	4	24755	4	–1.18	1.18(7)	–1.21	1.11(7)
600.6331	13374	8	30018	7	–0.13	1.33(8)	–0.18	1.18(8)
606.1239	10030	7	26524	6	–1.35	7.84(6)	–1.34	8.00(6)
611.0572	10163	6	26524	6	–1.48	5.87(6)	–1.47	5.99(6)
611.4381	13374	8	29724	8	–0.32	8.16(7)	–0.28	8.84(7)
619.7452	10730	6	26861	7	–0.72	3.08(7)	–0.67	3.45(7)
620.0823	11006	7	27128	8	–1.14	1.17(7)	–1.22	9.61(6)
620.5635	10117	4	26227	4	–1.66	3.36(6)	–1.75	2.74(6)
627.8676	9647	6	25569	7	–0.86	2.17(7)	–0.88	2.10(7)
630.5264	11006	7	26861	7	–1.05	1.41(7)	–1.00	1.58(7)
631.8115	7438	5	23261	5	–1.36	6.78(6)	–1.30	7.85(6)
635.7227	10117	4	25842	5	–1.76	2.71(6)	–1.70	3.10(6)
636.3633	9045	3	24755	4	–1.22	9.60(6)	–1.25	9.00(6)

Table 4. *Continued.*

λ[a] (nm)	Lower level[b] cm^{-1}	J	Upper level[b] cm^{-1}	J	log gf HFR[c]	gA HFR[c]	log gf (nm)	gA cm^{-1}
636.3823	11419	7	27128	8	–1.15	1.11(7)	–1.23	9.12(6)
637.6219	10163	6	25842	5	–1.85	2.29(6)	–1.79	2.62(6)
639.7707	9129	4	24755	4	–1.97	1.67(6)	–2.00	1.57(6)
639.7973	8490	5	24116	6	–0.78	2.49(7)	–0.94	1.73(7)
643.9129	11448	5	26973	5	–1.69	3.24(6)	–1.65	3.55(6)
644.2162	11006	7	26524	6	–1.31	7.66(6)	–1.30	7.82(6)
647.2073	10163	6	25610	6	–0.96	1.50(7)	–0.87	1.86(7)
647.3876	11419	7	26861	7	–1.08	1.27(7)	–1.03	1.42(7)
648.9302	10163	6	25569	7	–1.87	2.02(6)	–1.89	1.95(6)
655.5609	11611	8	26861	7	–1.33	6.68(6)	–1.28	7.48(6)
659.3771	8100	4	23261	5	–1.66	3.13(6)	–1.60	3.62(6)
663.1100	11448	5	26524	6	–1.72	3.12(6)	–1.71	3.18(6)
663.1945	10536	5	25610	6	–1.64	3.50(6)	–1.54	4.35(6)
663.5378	11794	7	26861	7	–1.34	6.56(6)	–1.29	7.34(6)
665.6833	14706	9	29724	8	0.27	2.66(8)	0.31	2.88(8)
684.5255	11006	7	25610	6	–0.92	1.43(7)	–0.82	1.78(7)
704.4439	11419	7	25610	6	–1.04	1.05(7)	–0.94	1.30(7)
705.8969	11448	5	25610	6	–1.62	2.99(6)	–1.52	3.71(6)
722.7694	13029	8	26861	7	–1.62	2.96(6)	–1.57	3.31(6)
741.2319	13374	8	26861	7	–1.79	1.84(6)	–1.75	2.06(6)

[a] Wavelengths in air are deduced from experimental excitation energies complied by Martin *et al.* [21], [b] each level is represented by its experimental value and its J-value as compiled in the NIST tables [21]. All the lower levels are odd and all the upper levels are even, [c] computed using the HFR model (see text), [d] HFR values normalized using the radiative lifetimes measured in the present work.

More precisely, among the 20 levels appearing in Table 2, those situated at 22 571.48, 22 675.44, 23 660.20, 26 961.96, 27 198.24 and 28 508.79 cm^{-1} were excluded from the Table 4 for the reasons mentioned above.

In their paper, Scholl *et al.* [14] also deduced f-values from their measured lifetimes combined with experimental branching fractions published by Lage and Whaling [10] and Goly *et al.* [11]. When comparing these results with the 'normalized' oscillator strengths obtained in the present work, a satisfactory general agreement was found as shown in Figure 1. In fact, the mean ratio between both sets of gf-values, gf (this work)/gf [14], was found to be equal to 1.31 ± 0.76 when considering all the 32 transitions common to both works but was reduced to 0.99 ± 0.31 when excluding the lines at 538.126 and 473.417 nm for which very large discrepancies were observed. These two transitions originate from the levels at 22 675.44 and 24 115.50 cm^{-1} for which the HFR lifetimes disagree considerably from the laser measurements (see Tab. 2).

The new set of transition probabilities obtained in the present work and summarized in Table 4 is expected to help the astrophysicists in their analysis of the chemical composition of CP stars. These results will be incorporated in the database DREAM accessible at the web site: `http://www.umh.ac.be/~astro/dream.shtml`.

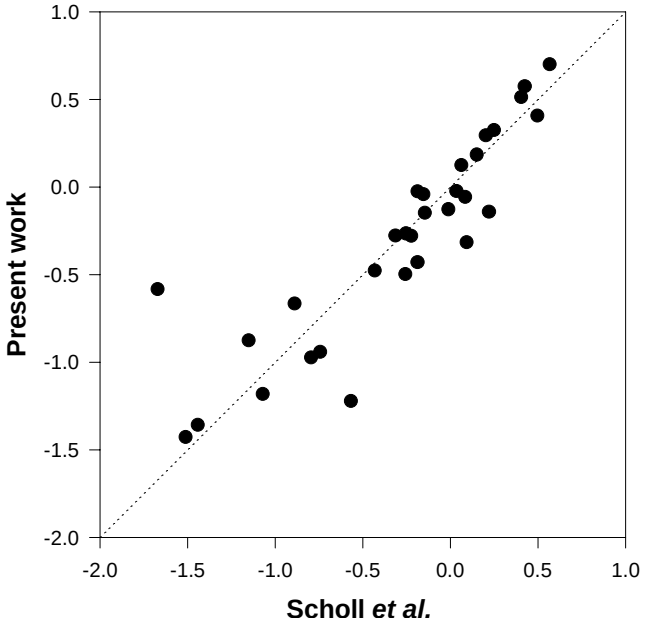

Fig. 1. Comparison of the oscillator strengths ($\log gf$) obtained in the present work (normalized values) with those obtained by Scholl *et al.* [14]. The dotted line corresponds to a perfect agreement between the two sets of data. For more details, see also the text.

This work was financially supported by the Swedish Research Council and by the EU-IHP Access to Research Infrastructures Program (contract HPRI-CT-1999-00041). Financial support from the Belgian FNRS and FRIA is acknowledged by E.B. and P.Q. and by P.-H.L., respectively. E.B., P-H.L. and P.Q. would like also to thank the kind hospitality enjoyed during their different stays at the Lund Laser Centre.

References

1. L. Dolk, G.M. Wahlgren, H. Lundberg, Z.S. Li, U. Litzén, S. Ivarsson, I. Ilyin, S. Hurbig, Astron. Astrophys. **385**, 111 (2002)
2. C. Sneden, A. McWilliam, G.W. Preston, J.J Cowan, D.L. Burris, B.J. Armosky, Astrophys. J. **467**, 819 (1996)
3. N. Grevesse, G. Blanquet, Solar Phys. **8**, 5 (1969)
4. V.N. Gorshkov, V.A. Komarovskii, Sov. Astron. AJ **30**, 333 (1986)
5. C.R. Cowley, T. Ryabchikova, F. Kupka, D.J. Bord, G. Mathys, W.P. Bidelman, Mon. Not. R. Astron. Soc. **317**, 299 (2000)
6. E. Biémont, P. Quinet, Phys. Scripta **T105**, 38 (2003)
7. C.H. Corliss, W.R. Bozman, *Experimental transition probabilities for spectral lines of seventy elements*, Nat. Bur. Stand. (U.S.), Monogr. 53 (1962)
8. T. Andersen, G. Sorensen, Sol. Phys. **38**, 343 (1974)
9. T. Andersen, O. Poulsen, P.S. Ramanujam, A. Petrakiev Petkov, Sol. Phys. **44**, 257 (1975)
10. C.S. Lage, W. Whaling, J. Quant. Spectrosc. Radiat. Transfer **16**, 537 (1976)
11. A. Goly, J. Kusz, N.B. Quang, S. Weniger, J. Quant. Spectrosc. Radiat. Transfer **45**, 157 (1991)
12. V.N. Gorchkov, V.A. Komarovskii, Opt. Spectrosc. **58**, 561 (1985)
13. K.B. Blagoev, V.A. Komarovskii, At. Data Nucl. Data Tables **56**, 1 (1994)
14. T.J. Scholl, R.A. Holt, D. Masterman, R.C. Rivest, S.D. Rosner, A. Sharikova, Can. J. Phys. **80**, 713 (2002)
15. E. Biémont, H.P. Garnir, P. Palmeri, P. Quinet, Z.S. Li, Z.G. Zhang, S. Svanberg, Phys. Rev. A **64**, 022503 (2001)
16. P. Palmeri, P. Quinet, Y. Frémat, J.-F. Wyart, E. Biémont, Astrophys. J. Suppl. **129**, 367 (2000)
17. A. Ginibre, Phys. Scripta **39**, 694 (1989)
18. A. Ginibre, Phys. Scripta **39**, 710 (1989)
19. B. Fuurman, D. Stefanska, E. Stachowska, J. Ruczkowski, J. Dembczynski, Eur. Phys. J. D **17**, 275 (2001)
20. Li Maosheng, Ma Hongliang, Chen Miaohua, Lu Fuquan, Tang Jiayong, Yang Fujia, Phys. Rev. A **62**, 052504-1 (2000)
21. W.C. Martin, R. Zalubas, L. Hagan, *Atomic Energy Levels – The Rare Earth Elements*, NBS-NSRDS 60, US Dept of Commerce, Washington DC (1978)
22. H.L. Xu, Z.K. Jiang, Z.G. Zhang, Z.S. Dai, S. Svanberg, P. Quinet, E. Biémont, J. Phys. B **36**, 1771 (2003)
23. R.D. Cowan, *The Theory of Atomic Structure and Spectra* (Univ. California Press, Berkeley, 1981)
24. L. Brewer, J. Opt. Soc. Am. **61**, 1666 (1971)